EURASIP Journal on
Wireless Communications and Networking
a SpringerOpen Journal

RESEARCH Open Access

What should be fed back for per-cell codebook-based limited feedback coordinated multi-point systems?

Di Su* and Chenyang Yang

Abstract

Per-cell codebook-based limited feedback is highly desirable in coordinated multi-point (CoMP) systems owing to flexibility and compatibility. Except for the per-cell codeword indices, each user should feed back other information for the central unit to reconstruct global channel direction information (CDI) and estimate channel quality information (CQI) for downlink transmission. In this paper, we analyze the essential feedback information for per-cell codebook-based coherent CoMP systems. To show what should be fed back to estimate the CQI, we first derive a conservative CQI estimation to avoid the outage in transmission, which depends on the quantization accuracy and the norm of the global channel. We then analyze whether the per-cell small-scale fading channel norms are necessary to feed back in obtaining the global channel norm and reconstructing the global CDI. Next, we analyze whether the feedback of phase ambiguity (PA) is necessary. Both the analysis and simulation results show that the global channel norm should be fed back instead of the per-cell channel norms. The benefit of the PA feedback is evident only when the number of base stations is large and the number of antennas at each base station is small.

1 Introduction

Coordinated multi-point (CoMP) transmission has drawn broad attention recently [1,2]. When all the coordinated base stations (BSs) share both data and channel information, coherent cooperative transmission, also known as joint transmission, can provide high spectral efficiency for cellular systems if the BSs can obtain high-quality channels. This however requires large feedback overhead for frequency division duplexing (FDD) CoMP systems. Though CoMP has various forms, depending on the information shared among the BSs, we refer coherent cooperative transmission as CoMP in the rest of the paper for simplicity.

Limited feedback techniques are widely applied in reporting channel information to the BS in multi-input-multi-output (MIMO) systems and have been extensively studied [3]. To facilitate downlink beamforming, each user needs to feed back quantized channel direction information (CDI) to the BS. To provide the essential information for spatial scheduling and modulation and coding selection (MCS), each user needs to feed back the estimated channel quality information (CQI) to the BS, which should be signal-to-noise and interference ratio (SINR) in multi-user MIMO (MU-MIMO) systems [4].

Despite that CoMP systems can be viewed as a large MIMO system with a super BS, there are many subtle but critical differences in terms of system setting and channel feature. As a result, the well-explored techniques developed for single-cell MIMO systems cannot be extended to CoMP systems in a straightforward manner.

The CoMP channel is composed of multiple single-cell channels between the coordinated BSs and each user. The coordinated cluster may be formed dynamically [2]. Consequently, in applying vector quantization theory to design a global codebook for quantizing the global CDI of the CoMP channel, there is lack of flexibility and compatibility [5]. It is more desirable to design a per-cell codebook-based feedback scheme, where each single-cell CDI is first quantized with a codebook, and then the global CDI is reconstructed with the quantized per-cell

*Correspondence: disu@ee.buaa.edu.cn
School of Electronics and Information Engineering, Beihang University, Beijing 100191, People's Republic of China

Springer

© 2013 Su and Yang; licensee Springer. This is an Open Access article distributed under the terms of the Creative Commons Attribution License (http://creativecommons.org/licenses/by/2.0), which permits unrestricted use, distribution, and reproduction in any medium, provided the original work is properly cited.

CDIs. Such a feedback scheme is suboptimal in nature. Nonetheless, its performance can be improved significantly by judiciously designing the methods for the codeword selection [5,6], global CDI reconstruction [7], and bit allocation among the per-cell codebooks [6,8]. When the independent codeword selection is applied, which is a codeword selection method extended from the single cell MIMO systems, phase ambiguity (PA) will lead to severe performance degradation [7]. Fortunately, when the PA is quantized and fed back, the performance of CoMP systems will be largely retrieved [8]. This will however introduce extra feedback overhead.

To assist downlink scheduling and MCS, the CQI should be available at the BS side, also in the form of SINR for CoMP systems. CQI estimation has a large impact on system performance. An optimistic estimate will lead to the outage in the downlink transmission. To help each user estimate the SINR accurately, full multiplexing spatial scheduling and equal power allocating among the selected users are usually assumed [4,9]. However, to meet the per-BS power constraint (PBPC) of CoMP system, the powers allocated to the users are not necessarily equal and unknown at the users. Therefore, the CQI is no longer able to be estimated accurately at each user. Instead, the BSs should estimate the SINRs experienced at the users' end, and each user should feed back necessary information to its master BS for CQI estimation.

In this paper, we strive to answer the following question: what is the essential feedback information for the estimation of CQI and the reconstruction of global CDI at the BSs in CoMP systems? Single stream transmission is considered to simplify the analysis. To analyze what should be fed back for CQI estimation, we first derive a method to estimate the SINR to avoid the outage in downlink transmission. Then, we analyze the necessity of feeding back the per-cell small-scale fading channel norms by comparing the average quantization performance of the global channel norm and the asymptotic weighting factors in the global CDI with and without the per-cell channel norm feedback. We proceed to analyze the necessity of feeding back the PA by comparing the average quantization performance with and without the PA feedback. Finally, we use numerical and simulation results to validate the analysis and show whether the per-cell channel norms and the PA should be fed back in typical settings.

Notations: The conjugate transpose of a vector (or matrix) is denoted by $(\cdot)^H$. The Euclidean norm is represented by $\|\cdot\|$, and the magnitude of a complex variable is by $|\cdot|$. The $N \times M$ complex matrixes are denoted by $\mathbb{C}^{N\times M}$. $\mathcal{CN}(b,N)$ denotes the complex Gaussian distribution with mean b and covariance N. $\mathbf{I}$ denotes the identity matrix, and $diag\{\cdot\}$ is a diagonal matrix. $\mathbb{E}\{\cdot\}$ denotes the expectation operator.

2 System model

2.1 CoMP channel model

Consider a coherent downlink CoMP system with universal frequency reuse, where N_c BSs each equipped with n_t antennas cooperatively transmit to M single antenna users. The coordinated BSs are connected to a central unit (CU) via backhaul links with unlimited capacity and zero latency.

The downlink global channel of each user, say the mth user, is composed of all the per-cell channels from each coordinated BS to the user, which can be represented by

$$\mathbf{g}_m = \left[\alpha_{m,1}\mathbf{h}_{m,1}^H, \ldots, \alpha_{m,N_c}\mathbf{h}_{m,N_c}^H\right]^H = \mathbf{R}_m^{\frac{1}{2}}\mathbf{h}_m, \tag{1}$$

where $\alpha_{m,n}$ is the large-scale fading gain including the path loss and shadowing, $\mathbf{h}_{m,n} \in \mathbb{C}^{n_t\times 1}$ is the small-scale fading channel vector from the nth coordinated BS to the mth user, $\mathbf{h}_m = \left[\mathbf{h}_{m,1}^H, \ldots, \mathbf{h}_{m,N_c}^H\right]^H$ is the concatenated small-scale fading channel, and $\mathbf{R}_m = diag\left\{\alpha_{m,1}^2\mathbf{I}_{n_t}, \ldots, \alpha_{m,N_c}^2\mathbf{I}_{n_t}\right\}$ is the covariance matrix, which reflects the spatial correlation of the global channel and depends on the user location. To simplify the analysis and highlight the feature of CoMP channels, we assume that the per-cell channels $\mathbf{h}_{m,n}, n = 1,\ldots N_c, m = 1,\ldots,M$ are independent and identically distributed (i.i.d.), and each of their entry is subject to $\mathcal{CN}(0,1)$. It is shown that Equation 1 resembles Kronecker's spatially correlated channel model.

The norm of the global channel is

$$||\mathbf{g}_m|| = \sqrt{\sum_{n=1}^{N_c}\alpha_{m,n}^2||\mathbf{h}_{m,n}||^2}, \tag{2}$$

and the CDI of the global channel is

$$\bar{\mathbf{g}}_m \triangleq \frac{\mathbf{g}_m}{\|\mathbf{g}_m\|} = [g_{m,1}\bar{\mathbf{h}}_{m,1}^H, \ldots, g_{m,N_c}\bar{\mathbf{h}}_{m,N_c}^H]^H, \tag{3}$$

where $\bar{\mathbf{h}}_{m,n} \triangleq \frac{\mathbf{h}_{m,n}}{\|\mathbf{h}_{m,n}\|}$ is the nth per-cell CDI vector and

$$g_{m,n} = \frac{\alpha_{m,n}\|\mathbf{h}_{m,n}\|}{\|\mathbf{g}_m\|} = \frac{\alpha_{m,n}\|\mathbf{h}_{m,n}\|}{\sqrt{\sum_{n=1}^{N_c}\alpha_{m,n}^2\|\mathbf{h}_{m,n}\|^2}} \tag{4}$$

is a weighting factor, which reflects the contribution of the per-cell CDI to the global CDI, and $\|\mathbf{h}_{m,n}\|$ is the per-cell small-scale fading channel norm.

2.2 Per-cell codebook-based global CDI feedback

With the per-cell codebook-based limited feedback scheme, the per-cell codebooks are used to quantize the

per-cell CDI vectors. That is to say, each user selects the codewords for N_c per-cell CDI vectors, then feeds back the indices of these codewords to the CU. The global CDI vector for each user is reconstructed at the CU. Assume that the large-scale fading gains are perfectly known at the CU. In practice, they can be obtained by averaging the downlink receive signal energy at each user and feeding back to the CU, which needs low feedback overhead.

2.2.1 Reconstruction of the global CDI

After receiving the indices of the selected codewords for multiple per-cell CDI vectors from each user, $\{j_1, \ldots, j_{N_c}\}$, we can reconstruct the global CDI of the mth user at the CU only with the large-scale fading gains, which is

$$\hat{\mathbf{g}}_m = \left[\hat{g}_{m,1}\mathbf{c}_{m,j_1}^H, \ldots, \hat{g}_{m,N_c}\mathbf{c}_{m,j_{N_c}}^H\right]^H, \tag{5}$$

where $\mathbf{c}_{m,j_n}$ represents the selected codeword from the nth per-cell codebook $\mathcal{C}_n$ for quantizing $\bar{\mathbf{h}}_{m,n}$ and

$$\hat{g}_{m,n} = \frac{\alpha_{m,n}}{\sqrt{\sum_{n=1}^{N_c}\alpha_{m,n}^2}}, \tag{6}$$

is the estimated weighting factor.

The quantization accuracy of the reconstructed global CDI for user m is expressed as

$$\cos^2\theta_m = |\bar{\mathbf{g}}_m^H\hat{\mathbf{g}}_m|^2 = \left|\sum_{n=1}^{N_c} g_{m,n}\hat{g}_{m,n}\bar{\mathbf{h}}_{m,n}^H\mathbf{c}_{m,j_n}\right|^2, \tag{7}$$

since the difference in phase between the reconstructed global CDI $\hat{\mathbf{g}}_m$ and the actual global CDI $\bar{\mathbf{g}}_m$ does not affect the performance [3]. The quantization accuracy is associated with the *Grassmann choral distance* [3], which is $1 - \cos^2\theta_m$. The quantization accuracy of the reconstructed global CDI is referred to as 'global quantization accuracy' for short in the sequel.

Remark 1. If the per-cell small-scale fading norms $||\mathbf{h}_{m,n}||$, $n = 1, \ldots, N_c$ are perfectly known at the CU, the global CDI can be reconstructed with Equation 5 but replacing $\hat{g}_{m,n}$ by $g_{m,n}$. Then, the global quantization accuracy becomes

$$\cos^2\theta_m = \left|\sum_{n=1}^{N_c} g_{m,n}^2\bar{\mathbf{h}}_{m,n}^H\mathbf{c}_{m,j_n}\right|^2. \tag{8}$$

2.2.2 Codeword selection

Per-cell codewords can be selected either independently or jointly according to different criteria at the user side. The criteria depend on the method to reconstruct the global CDI, which determines the global quantization accuracy. Here, we assume that the global CDI is reconstructed with Equation 5. Two popular codeword selection methods are shown as follows:

- *Joint codeword selection.* Each user jointly selects the per-cell codewords to maximize its global quantization accuracy, i.e.,

$$\begin{aligned}&\arg\max_{j_1,\ldots,j_{N_c}} \cos^2\theta_m \\ &= \arg\max_{j_1,\ldots,j_{N_c}} \left|\sum_{n=1}^{N_c} g_{m,n}\hat{g}_{m,n}\bar{\mathbf{h}}_{m,n}^H\mathbf{c}_{m,j_n}\right|^2.\end{aligned} \tag{9}$$

  This codeword selection method requires prohibited complexity for exhaustive searching multiple codewords. Nonetheless, the complexity can be remarkably reduced, e.g., with a serial codeword searching algorithm proposed in [6].
- *Independent codeword selection.* Each user independently selects the per-cell codewords to maximize the quantization accuracy of each per-cell CDI vector, i.e.,

$$\arg\max_{j_n} |\bar{\mathbf{h}}_{m,n}^H\mathbf{c}_{m,j_n}|, n = 1, \ldots, N_c. \tag{10}$$

  This method suffers from severe performance degradation, especially when $\alpha_{m,1} = \ldots = \alpha_{m,N_c}$, which comes from the PAs, $e^{j\xi_{m,n}} = \frac{\mathbf{h}_{m,n}^H\mathbf{c}_{m,j_n}}{|\mathbf{h}_{m,n}^H\mathbf{c}_{m,j_n}|}$, $n = 1, \ldots, N_c$ [8]. Nevertheless, the performance can be significantly retrieved by feeding back the PAs as shown in [7].

3 Feedback for CQI

When the CU obtains the global CDIs from multiple users, it can compute the joint beamforming matrix for downlink cooperative transmission. To facilitate user scheduling as well as the power allocation and MCS for the selected users, the CU also needs to estimate the CQI of each user, which is the SINR experienced at the user's end [4].

In limited feedback MU-MIMO systems, each user only knows its own channel but is unaware of the beamforming vectors for other users, while the BS knows all the beamforming vectors but does not know the actual downlink channels of users. As a result, neither each user nor the BS can accurately compute the downlink SINR experienced by the user.

One popular approach to solve this problem is the orthogonal beamforming-based limited feedback, e.g., per user unitary and rate control (PU2RC) [9], where the beamforming vectors are selected from an orthonormal codebook. Since both the BS and each user know that the beamforming vectors of scheduled users are orthogonal and with unit norm, the SINR can be estimated at

the user's end accurately if the number of selected users equals to n_t, i.e., full multiplexing is achieved. Note that the PU2RC implicitly assumes that the transmit power is equally allocated to the users.

In order to borrow the idea of PU2RC, we consider a transmission scheme using semi-orthogonal user scheduling (SUS) [4] and zero-forcing beamforming, which is asymptotically optimal in terms of sum rate in single-cell systems. If the orthogonal threshold in SUS is small and the power is equally allocated among the selected users, such a scheme will resemble the PU2RC. However, in CoMP systems, the PBPC may not be met with the equal power allocation. When considering the power allocation under the PBPC, each user does not know the power allocated to it. This suggests that we need to estimate the SINR at the CU for CoMP systems.

If we assume that the threshold in SUS equals to zero, we have $\hat{\mathbf{g}}_i^H \hat{\mathbf{g}}_m = 0, \forall i \neq m$. Then, the beamforming vector for the mth user $\mathbf{w}_m = \hat{\mathbf{g}}_m^H$, and the SINR can be obtained as

$$\begin{aligned} \mathrm{SINR}_m &= \frac{p_m ||\mathbf{g}_m||^2 |\bar{\mathbf{g}}_m^H \mathbf{w}_m|^2}{\sigma_m^2 + ||\mathbf{g}_m||^2 \sum_{i\neq m}^{\bar{M}} p_i |\bar{\mathbf{g}}_m^H \mathbf{w}_i|^2} \\ &= \frac{p_m ||\mathbf{g}_m||^2 \cos^2\theta_m}{\sigma_m^2 + p_m ||\mathbf{g}_m||^2 \sum_{i\neq m}^{\bar{M}} \rho_i |\bar{\mathbf{g}}_m^H \hat{\mathbf{g}}_i|^2}, \end{aligned} \tag{11}$$

where p_m is the power allocated to user m, σ_m^2 is the variance of noise and inter-cluster interference at the user, and $\bar{M}$ is the number of scheduled users. $\rho_i \triangleq \frac{p_i}{p_m}$ reflects that the allocated powers to different users may differ, especially when the PBPC is considered.

The relationship of the true value and the quantized global CDI can be described as $\bar{\mathbf{g}}_m = \cos\theta_m \hat{\mathbf{g}}_m + \sin\theta_m \mathbf{s}_m$, where $\cos\theta_m$ is the global quantization accuracy and $\mathbf{s}_m$ is a unitary vector with $\mathbf{s}_m^H \hat{\mathbf{g}}_m = 0$. Upon substituting into Equation 11, the SINR can be rewritten as

$$\begin{aligned} &\mathrm{SINR}_m \\ &= \frac{p_m ||\mathbf{g}_m||^2 \cos^2\theta_m}{\sigma_m^2 + p_m ||\mathbf{g}_m||^2 \sum_{i\neq m}^{\bar{M}} \rho_i |\cos\theta_m \hat{\mathbf{g}}_m^H \hat{\mathbf{g}}_i + \sin\theta_m \mathbf{s}_m^H \hat{\mathbf{g}}_i|^2} \\ &= \frac{p_m ||\mathbf{g}_m||^2 \cos^2\theta_m}{\sigma_m^2 + p_m ||\mathbf{g}_m||^2 \sin^2\theta_m \sum_{i\neq m}^{\bar{M}} \rho_i |\mathbf{s}_m^H \hat{\mathbf{g}}_i|^2}. \end{aligned} \tag{12}$$

Note that the vector $\mathbf{s}_m$ has the same size with the global CDI $\bar{\mathbf{g}}_m$. This means that the required overhead for feeding back such a vector will be the same as that for the global CDI. Therefore, we proceed to analyze how to estimate the SINR at the CU without knowing $\mathbf{s}_m$. To this end, we estimate the term $I_m \triangleq \sum_{i\neq m}^{\bar{M}} \rho_i |\mathbf{s}_m^H \hat{\mathbf{g}}_i|^2$ in the denominator of the SINR, which can be derived as

$$\begin{aligned} I_m &= \sum_{i\neq m}^{\bar{M}} \rho_i \mathbf{s}_m^H \hat{\mathbf{g}}_i \hat{\mathbf{g}}_i^H \mathbf{s}_m \\ &= \mathbf{s}_m^H \left(\sum_{i\neq m}^{\bar{M}} \rho_i \hat{\mathbf{g}}_i \hat{\mathbf{g}}_i^H \right) \mathbf{s}_m = \mathbf{s}_m^H \mathbf{G}_m \mathbf{s}_m, \end{aligned} \tag{13}$$

where $\mathbf{G}_m \triangleq \sum_{i\neq m}^{\bar{M}} \rho_i \hat{\mathbf{g}}_i \hat{\mathbf{g}}_i^H$.

When an optimistic SINR estimate is used for MCS, the outage will occur in the downlink transmission. To reduce the outage probability, we try to find a conservative estimation of the SINR. This is equivalent to finding the maximal possible value of I_m by solving the optimization problem as follows:

$$\begin{aligned} &\max_{\mathbf{s}_m} I_m \\ &s.t. ||\mathbf{s}_m||^2 = 1, \end{aligned} \tag{14}$$

which is a convex optimization problem.

From the Karush-Kuhn-Tucker (KKT) condition, the optimal solution $\mathbf{s}_m^{\mathrm{op}}$ of Equation 14 should ensure that the Lagrangian function $\mathcal{L}(\mathbf{s}_m, \lambda)$ meets $\frac{\partial \mathcal{L}(\mathbf{s}_m,\lambda)}{\partial \mathbf{s}_m}|_{\mathbf{s}_m=\mathbf{s}_m^{\mathrm{op}}} = 0$, where $\mathcal{L}(\mathbf{s}_m, \lambda) = \mathbf{s}_m^H \mathbf{G}_m \mathbf{s}_m - \lambda \mathbf{s}_m^H \mathbf{s}_m$ with λ representing the Lagrange multiplier. As a result, its solution $\mathbf{s}_m^{\mathrm{op}}$ should meet the equation $\mathbf{G}_m \mathbf{s}_m^{\mathrm{op}} = \lambda \mathbf{s}_m^{\mathrm{op}}$. It indicates that $\mathbf{s}_m^{\mathrm{op}}$ is an eigenvector of $\mathbf{G}_m$. To find the maximal value of I_m, $I_m^{\max}$, $\mathbf{s}_m^{\mathrm{op}}$ should be the eigenvector corresponding to the maximal eigenvalue, i.e., $\mathbf{G}_m \mathbf{s}_m^{\mathrm{op}} = \lambda_m^{\max} \mathbf{s}_m^{\mathrm{op}}$, where $\lambda_m^{\max}$ is the maximal eigenvalue of $\mathbf{G}_m$. Then, $I_m^{\max} = (\mathbf{s}_m^{\mathrm{op}})^H \mathbf{G}_m \mathbf{s}_m^{\mathrm{op}} = \lambda_m^{\max} (\mathbf{s}_m^{\mathrm{op}})^H \mathbf{s}_m^{\mathrm{op}} = \lambda_m^{\max}$.

The SINR can be estimated conservatively at the CU as

$$\widehat{\mathrm{SINR}}_m = \frac{p_m ||\mathbf{g}_m||^2 \cos^2\theta_m}{\sigma_m^2 + p_m ||\mathbf{g}_m||^2 \sin^2\theta_m \lambda_m^{\max}}. \tag{15}$$

The value of $\lambda_m^{\max}$ can be computed at the CU, which depends on the quantized global CDIs of the co-scheduled users of user m, $\hat{\mathbf{g}}_i, \forall i \neq m$, and the allocated powers to the users, $p_i, i = 1, \ldots, \bar{M}$.

Remark 2. If the transmit power is allocated equally to the selected users, we have $\rho_i = 1, \forall i \neq m$. Then, it is not hard to show that $\mathbf{G}_m = \sum_{i\neq m}^{\bar{M}} \hat{\mathbf{g}}_i \hat{\mathbf{g}}_i^H$ meets $\mathbf{G}_m^2 = \mathbf{G}_m$, which suggests $\mathbf{G}_m$ is an idempotent matrix. As analyzed in [10], the eigenvalue of an idempotent matrix is either 0 or 1. In this case, $I_m^{\max} = \lambda_m^{\max} = 1$, and Equation 15 becomes

$$\widehat{\mathrm{SINR}}_m = \frac{p_m ||\mathbf{g}_m||^2 \cos^2\theta_m}{\sigma_m^2 + p_m ||\mathbf{g}_m||^2 \sin^2\theta_m},$$

which is the same as the CQI estimate in PU2RC [9]. It implies that the derived method is an extension of the popular method in single-cell systems, where the estimated CQI is accurate with the full multiplexing scheduling [9].

Remark 3. Although the CQI estimation for CoMP transmission is conservative, it does not mean that non-CoMP will outperform the CoMP transmission, as will be shown by simulations later. This is because in non-CoMP systems, the CQI is also estimated conservatively for prevalent FDD systems for the same reason of avoiding the outage [9]. It is worthy to note that in many practical systems, hybrid automatic repeat request (HARQ) will be employed when outage occurs. Nonetheless, HARQ requires extra time for retransmission, which leads to the reduction of the overall spectral efficiency. Consequently, the CQI estimation is usually conservative even when considering HARQ in order to reduce the outage probability.

It is shown from Equation 15 that each user, say user m, needs to feed back the global channel norm $||\mathbf{g}_m||^2$, the noise and inter-cluster interference variance σ_m^2, the quantized global CDI $\hat{\mathbf{g}}_m$, as well as the global quantization accuracy $\cos\theta_m$ to the CU for estimating the CQI. In practice, we only need to feed back the quantized version of $\frac{||\mathbf{g}_m||^2}{\sigma_m^2}$, $\mathbf{g}_m$, and $\cos\theta_m$. As will be shown later, the value of σ_m^2 does not affect our forthcoming analysis; we assume $\sigma_m^2 = 1$ in the analytical analysis. In practice, σ_m^2 can be estimated at the user m by averaging the received signals then fed back to the CU, which does not need frequent feedback.

Since the large-scale fading gains are assumed known at the CU, we only need to consider the necessity of the feedback of per-cell small-scale fading norms, which are referred to as per-cell channel norms for short in the sequel.

4 Necessity of per-cell channel norm feedback

As shown in Equations 2 and 3, per-cell channel norms affect not only the norm but also the CDI of global channel by acting as the weighting factors. The global channel norm is a weighted sum of the per-cell norms, whose dimension is the same as that of the per-cell norm. The global CDI vector is an aggregation of the per-cell CDI vectors, whose dimension is N_c times that of the per-cell CDI. In this section, we analyze if the per-cell channel norms are necessary to be fed back for the estimation of the CQI and the reconstruction of the global CDI.

The CQI in Equation 15 only depends on the information of user m. Therefore, we omit the the subscript m for notation simplicity.

4.1 Necessity for global channel norm

For global CDI quantization, the per-cell codebook is more desirable since a global codebook is of high complexity, and lack of compatibility for a global channel with dynamic and large dimension. On contrary, for the global channel norm quantization used for estimating the CQI, we can either quantize the per-cell channel norms or the global channel norm. In the following, we analyze the performance of these two feedback mechanisms. Because $\frac{||\mathbf{g}_m||^2}{\sigma_m^2}$ should be fed back for estimating the CQI, we use the average quantization error of global channel energy, $\mathbb{E}[||\mathbf{g}||^2 - \widehat{||\mathbf{g}||^2}]$, as the performance metric, where $\widehat{||\mathbf{g}||^2}$ is obtained either from the quantized global channel norm or from the quantized per-cell channel norms.

4.1.1 Per-cell channel norm feedback

Denote the per-cell channel norm as $Y_n \triangleq \| \mathbf{h}_n \|$. The quantized version of Y_n is defined as the lower end of the quantization interval that includes Y_n, denoted as $\hat{Y}_n$, to ensure $\hat{Y}_n \leq Y_n$, which can avoid the outage led by optimistic estimation of channel norm and also simplify the analysis. The quantization procedure is

$$\hat{Y}_n = y^{(j)}, \quad \text{if} \quad y^{(j)} \leq Y_n < y^{(j+1)}, j = 1, \cdots, 2^{B_\mathrm{h}} \tag{16}$$

where $\{y^{(1)}, \ldots, y^{(2^{B_\mathrm{h}})}\}$ is the scalar codebook of size B_h for quantizing the per-cell channel norms and $y^{(2^{B_\mathrm{h}}+1)} \triangleq \infty$ [11]. Assume that Y_n is distributed within an interval with high probability, i.e., $\mathrm{P}[\delta_1 \leq Y_n \leq \delta_2] \approx 1$ [12]. Then, we can set $y^{(1)} = \delta_1$ and $y^{(2^{B_h})} = \delta_2$.

The global channel energy can be expressed as $\| \mathbf{g} \|^2 = \sum_{n=1}^{N_c} \alpha_n^2 Y_n^2$, and its reconstructed version from the per-cell channel norm feedback is $\widehat{\| \mathbf{g} \|^2} = \sum_{n=1}^{N_c} \alpha_n^2 \hat{Y}_n^2$. Then, its quantization performance is

$$\begin{aligned} \mathbb{E}\left[\| \mathbf{g} \|^2 - \widehat{\| \mathbf{g} \|^2} \right] &= \mathbb{E}\left[\sum_{n=1}^{N_c} \alpha_n^2 (Y_n^2 - \hat{Y}_n^2) \right] \\ &= \sum_{n=1}^{N_c} \alpha_n^2 (\mathbb{E}[Y_n^2] - \mathbb{E}[\hat{Y}_n^2]). \end{aligned} \tag{17}$$

Because we assume $\mathrm{P}[\delta_1 \leq Y_n \leq \delta_2] \approx 1$ and $\mathrm{P}[Y_n \leq \delta_1] \approx 0$, we obtain

$$\mathbb{E}[Y_n^2] = \int_0^\infty y^2 f(y) \mathrm{d}y \approx \sum_{j=1}^{2^{B_\mathrm{h}}} \int_{y^{(j)}}^{y^{(j+1)}} y^2 f(y) \mathrm{d}y,$$

$$\mathbb{E}[\hat{Y}_n^2] = \sum_{j=1}^{2^{B_\mathrm{h}}} \int_{y^{(j)}}^{y^{(j+1)}} (y^{(j)})^2 f(y) \mathrm{d}y,$$

where $f(y)$ is the probability distribution function of the per-cell channel norm Y_n, and then

$$\mathbb{E}[Y_n^2] - \mathbb{E}[\hat{Y}_n^2] \approx \sum_{j=1}^{2^{B_\mathrm{h}}} \int_{y^{(j)}}^{y^{(j+1)}} \left[y^2 - (y^{(j)})^2 \right] f(y) \mathrm{d}y.$$

To simplify the analysis and gain some useful insights, we consider the case of high-resolution quantization as in [12], where the quantization interval, $y^{(j+1)} - y^{(j)}$, is very small.

Proposition 1. *When the codebook size B_h is very large,*

$$\mathbb{E}[Y_n^2] - \mathbb{E}[\hat{Y}_n^2] \approx \frac{2(\delta_2 - \delta_1)}{2^{B_\mathrm{h}} - 1} \mathbb{E}[Y_n] + \frac{(\delta_2 - \delta_1)^2}{(2^{B_\mathrm{h}} - 1)^2}.$$

Proof. See Appendix 1. □

Upon substituting into Equation 17, we have

$$\mathbb{E}\left[\| \mathbf{g} \|^2 - \widehat{\| \mathbf{g} \|^2} \right] \approx \sum_{n=1}^{N_c} \frac{2\alpha_n^2(\delta_2 - \delta_1)}{2^{B_\mathrm{h}} - 1} \mathbb{E}[\| \mathbf{h}_n \|] + \sum_{n=1}^{N_c} \frac{\alpha_n^2(\delta_2 - \delta_1)^2}{(2^{B_\mathrm{h}} - 1)^2}, \tag{18}$$

which is accurate with large B_h. In fact, $B_\mathrm{h} \geq 4$ bits is enough for a good approximation.

4.1.2 Global channel norm feedback

Similar to Equation 16, the quantized version of the global channel norm is defined as

$$\widehat{\| \mathbf{g} \|} = x^{(j)}, \quad \text{if} \quad x^{(j)} \leq \| \mathbf{g} \| < x^{(j+1)}, j = 1, \cdots, 2^{B_\mathrm{g}} \tag{19}$$

where $\{x^{(1)}, \ldots, x^{(2^{B_\mathrm{g}})}\}$ is the scalar codebook of size B_g for quantizing the global channel norm, and $x^{(2^{B_\mathrm{g}}+1)} \triangleq \infty$.

Remind that $\mathrm{P}[\delta_1 \leq Y_n \leq \delta_2] \approx 1$ and $Y_n = \| \mathbf{h}_n \|$, from which we can obtain the distribution range of the global channel norm, $||\mathbf{g}|| = \sqrt{\sum_{n=1}^{N_c} \alpha_n^2 ||\mathbf{h}_n||^2}$, as

$$\mathrm{P}\left[\delta_1 \sqrt{\sum_{n=1}^{N_c} \alpha_n^2} \leq ||\mathbf{g}|| \leq \delta_2 \sqrt{\sum_{n=1}^{N_c} \alpha_n^2} \right] \approx 1. \tag{20}$$

Define $\Delta_1 \triangleq \delta_1 \sqrt{\sum_{n=1}^{N_c} \alpha_n^2}$ and $\Delta_2 \triangleq \delta_2 \sqrt{\sum_{n=1}^{N_c} \alpha_n^2}$. Then we can set $x^{(1)} = \Delta_1$ and $x^{(2^{B_\mathrm{g}})} = \Delta_2$, which implies that the codebook for global channel norm is location-dependent. Nonetheless, because the large-scale fading gains, $\alpha_n, n = 1, \ldots, N_c$, are assumed known to the CU, such a codebook can be generated at both the CU and the user by 'transforming' the codebook for per-cell channel norm by multiplying with $\sqrt{\sum_{n=1}^{N_c} \alpha_n^2}$ as shown in Equation 20.

Again, we consider a high-resolution quantization. In the same manner as in Proposition 1, we can derive the average quantization error of the global channel energy as

$$\begin{aligned} \mathbb{E}\left[\| \mathbf{g} \|^2 - \widehat{\| \mathbf{g} \|^2} \right] &\approx \frac{2(\Delta_2 - \Delta_1)}{2^{B_\mathrm{g}} - 1} \mathbb{E}[\| \mathbf{g} \|] + \frac{(\Delta_2 - \Delta_1)^2}{(2^{B_\mathrm{g}} - 1)^2} \\ &= \sqrt{\sum_{n=1}^{N_c} \alpha_n^2} \frac{2(\delta_2 - \delta_1)}{2^{B_\mathrm{g}} - 1} \mathbb{E}[\| \mathbf{g} \|] + \sum_{n=1}^{N_c} \alpha_n^2 \frac{(\delta_2 - \delta_1)^2}{(2^{B_\mathrm{g}} - 1)^2}, \end{aligned} \tag{21}$$

which is accurate when B_g is sufficiently large. In fact, $B_\mathrm{g} \geq 4$ bits is enough for a good approximation.

4.1.3 Comparison of the two feedback strategies

To compare the two channel norm feedback strategies, we first present a proposition, which shows the approximate relation between the average global norm and the average per-cell norm.

Proposition 2. *When the number of antennas at each BS n_t is large, we have* $\mathbb{E}[\| \mathbf{g} \|] \approx \sqrt{\sum_{n=1}^{N_c} \alpha_n^2} \times \mathbb{E}[||\mathbf{h}_n||]$.

Proof. See Appendix 2. □

In fact, this approximation is accurate even when $n_t = 2$. Upon substituting into Equation 21, we have

$$\mathbb{E}\left[\| \mathbf{g} \|^2 - \widehat{\| \mathbf{g} \|^2} \right] \approx \sum_{n=1}^{N_c} \frac{2\alpha_n^2(\delta_2 - \delta_1)}{2^{B_\mathrm{g}} - 1} \mathbb{E}[\| \mathbf{h}_n \|] + \sum_{n=1}^{N_c} \alpha_n^2 \frac{(\delta_2 - \delta_1)^2}{(2^{B_\mathrm{g}} - 1)^2}, \tag{22}$$

which is the same as (18) if $B_\mathrm{g} = B_\mathrm{h}$.

Note that the total number of bits for per-cell channel norm-based feedback is $N_c \times B_\mathrm{h}$ bits. This means that directly quantizing the global channel norm can achieve the same performance as quantizing the per-cell channel norms but with much less bits, when n_t is large.

One may wonder why this happens considering that the dynamic range of the global channel norm seems much larger than that of the per-cell channel norm from

Equation 20. Note that the global channel norm acts similarly to the variable $\sqrt{\sum_{n=1}^{N_c}\alpha_n^2}\times||\mathbf{h}_n||$ since they have the same dynamic range and expectation as shown in Equation 20 and Proposition 2. Be reminded that the assumption that the large-scale fading gains are perfectly known to the CU and each user. As a result, the quantization performance of the variable $\sqrt{\sum_{n=1}^{N_c}\alpha_n^2}\times||\mathbf{h}_n||$ is exactly the same as that of $||\mathbf{h}_n||$. This can also explain why the value of σ^2 does not affect our analysis regarding the channel norm feedback.

4.2 Necessity for global CDI

The global CDI depends on the per-cell channel norms as shown in Equation 4. If the per-cell channel norms are not fed back, we can employ the large-scale fading gains to reconstruct the global CDI as in Equation 5. The following proposition implies that using Equation 5 will lead to minor performance loss when the number of antennas at each BS is sufficiently large.

Proposition 3. *When $n_t\to\infty$, the weighting factor in global CDI g_n is approximately equal to that in the reconstructed global CDI $\hat{g}_n$, i.e., $g_n\approx\hat{g}_n$.*

Proof. See Appendix 3. □

Actually, the value of n_t does not need to be too large as will be shown in simulations. This suggests that the per-cell channel norms are unnecessary to be fed back for reconstructing the global CDI.

From the analysis, we can conclude that the per-cell channel norms are not necessary for feedback when n_t is large.

5 Necessity of PA feedback

The PA may have a large impact on the performance of per-cell codebook-based limited feedback coherent CoMP systems, depending on the methods of codeword selection, as analyzed in [13]. In this section, we investigate whether the PA feedback is necessary by comparing the performance with and without the PA feedback. As shown in [13], the performance gain of feeding back the PA with joint codeword selection is not significant, while the performance loss of not feeding back the PA with independent codeword selection is severe. Therefore, we consider the joint codeword selection for the strategy without the PA feedback and consider the independent codeword selection for the strategy with the PA feedback.

As analyzed in [8], the achievable data rate of each user in CoMP systems depends on the quantization accuracy of its global CDI. Hence, we employ the average quantization accuracy of global CDI, $\mathbb{E}[\cos^2\theta]$, as the performance metric for comparison and omit the subscript m for notation simplicity.

We consider the global CDI reconstruction method shown in Equation 5. Since the PA has the largest impact when $\alpha_1=\ldots=\alpha_{N_c}$ [7], we will consider this worst case in the analysis. In this case, the per-cell codebooks for quantizing the per-cell CDI vectors should have an identical size, say b_{CDI} bits. Then, the total bits for each user to quantize all the per-cell CDI vectors are $B_{\mathrm{CDI}}=N_c\times b_{\mathrm{CDI}}$ bits.

5.1 Quantization performance without PA feedback

For *joint codeword selection*, the per-cell codewords are selected according to Equation 9. In the case where $\alpha_1=\ldots=\alpha_{N_c}$, the global channel can be viewed as a channel of single cell MIMO system with a 'super BS' having N_cn_t transmit antennas. When we quantize this equivalent 'MIMO channel' with a globally generated codebook with the size of B_{CDI}, the average quantization accuracy is upper bounded by $1-2^{-\frac{B_{\mathrm{CDI}}}{N_cn_t-1}}$, which is tight when the global codebook is well designed and its size is sufficiently large [14]. Moreover, it was shown in [5, lemma 1] that when N_cn_t is large, the performance of the per-cell codebook-based feedback achieves the performance of the globally generated codebook. This suggests that the average global quantization accuracy without PA feedback is as follows:

$$A_{\mathrm{NPA}}\triangleq\mathbb{E}[\cos^2\theta|_{\mathrm{NPA}}]\approx 1-2^{-\frac{B_{\mathrm{CDI}}}{N_cn_t-1}}, \tag{23}$$

where $\cos^2\theta|_{\mathrm{NPA}}$ represents the quantization accuracy without PA feedback. This approximation is accurate when the following two conditions are met simultaneously: (1) the total number of feedback bits of each user is sufficient large, i.e., $B_{\mathrm{CDI}}\to\infty$, and (2) the value of $N_c\times n_t$ is sufficiently large.

5.2 Quantization performance with PA feedback

For *independent codeword selection*, the codewords for per-cell CDIs are selected according to Equation 10. Except for the B_{CDI} bits to quantize the CDI, we employ extra B_{PA} bits to quantize the PA. The codewords for quantizing the PA are selected according to the following criterion:

$$i_n^*=\arg\min_{i_n}|e^{j\xi_n}-c_{i_n}^{\xi}|,\forall n=1,\ldots,N_c \tag{24}$$

where $c_{i_n}^{\xi}$ is the i_nth codeword of the scalar codebook for the quantization of $e^{j\xi_n}$. Denote $e^{j\hat{\xi}_n}\triangleq c_{i_n^*}^{\xi}$ as the quantized PA and $e^{j\Delta\xi_n}\triangleq e^{j(\xi_n-\hat{\xi}_n)}$ is its quantization error.

Denote the quantization accuracy with PA feedback as $\cos^2\theta|_{\mathrm{PA}}$. Then the average global quantization accuracy with PA feedback can be derived as

$$\begin{aligned} A_{\mathrm{PA}} &\triangleq \mathbb{E}[\cos^2\theta|_{\mathrm{PA}}] = \mathbb{E}\Big[\frac{1}{\sqrt{N_c}}\Big|\sum_{n=1}^{N_c} g_n|\bar{\mathbf{h}}_n^H\mathbf{c}_{j_n}|e^{j(\Delta\xi_n)}\Big|^2\Big] \\ &= \mathbb{E}\Big[\frac{1}{N_c}\sum_{n=1}^{N_c} g_n^2|\bar{\mathbf{h}}_n^H\mathbf{c}_{j_n}|^2 \\ &+ \frac{2}{N_c}\sum_{n=1}^{N_c}\sum_{k>n}^{N_c} g_n|\bar{\mathbf{h}}_n^H\mathbf{c}_{j_n}||g_k|\bar{\mathbf{h}}_k^H\mathbf{c}_{j_k}|\cos(\Delta\xi_n-\Delta\xi_k)\Big]. \end{aligned} \tag{25}$$

Since the per-cell channel is complex Gaussian, its norm is independent with its direction vector. Then, g_n is independent from $\cos\theta_n$ and $e^{j\Delta\xi_n}$ because g_n depends on the per-cell channel norms, while $\cos\theta_n$ and $e^{j\Delta\xi_n}$ are associated with per-cell CDIs. Due to the isotropy nature of the per-cell CDI [15], $\cos\theta_n y$ and $e^{j\Delta\xi_n}$ are mutually independent. Further considering that per-cell channels are mutually independent, we know that g_n, $\cos\theta_n$, and $e^{j\Delta\xi_n}$ are independent of g_k, $\cos\theta_k$ and $e^{j\Delta\xi_k}$, $\forall n\neq k$. As a result, Equation 25 can be derived as

$$\begin{aligned} A_{\mathrm{PA}} &= \frac{1}{N_c}\sum_{n=1}^{N_c}\mathbb{E}[g_n^2]\times\mathbb{E}[\cos^2\theta_n] \\ &+ \frac{2}{N_c}\sum_{n=1}^{N_c}\sum_{k>n}^{N_c}\mathbb{E}[g_n]\,\mathbb{E}[g_k]\times\mathbb{E}[\cos\theta_n]\,\mathbb{E}[\cos\theta_k] \\ &\times\mathbb{E}[\cos(\Delta\xi_n-\Delta\xi_k)]. \end{aligned} \tag{26}$$

From Proposition 3, we know that

$$\mathbb{E}[g_n]\approx\hat{g}_n=\frac{1}{\sqrt{N_c}}, \tag{27}$$

which is accurate when n_t is sufficiently large.

Substituting Equation 27 into Equation 26, we have

$$\begin{aligned} A_{\mathrm{PA}} &\approx \frac{1}{N_c^2}\sum_{n=1}^{N_c}\mathbb{E}[\cos^2\theta_n] \\ &+ \frac{2}{N_c^2}\sum_{n=1}^{N_c}\sum_{k>n}^{N_c}\mathbb{E}[\cos\theta_n]\,\mathbb{E}[\cos\theta_k]\times\mathbb{E}[\cos(\Delta\xi_n-\Delta\xi_k)]. \end{aligned} \tag{28}$$

When the per-cell codebook is well designed and the codebook size is sufficiently large, the variance $\sigma^2_{\cos\theta_n}=\mathbb{E}[\cos\theta_n^2]-(\mathbb{E}[\cos\theta_n])^2$ will be small [16]. Then, $\mathbb{E}[\cos\theta_n]$ can be approximated by $\sqrt{\mathbb{E}[\cos\theta_n^2]}$, i.e.,

$$\mathbb{E}[\cos\theta_n]\approx\sqrt{1-2^{-\frac{B_{\mathrm{CDI}}}{N_c(n_t-1)}}}. \tag{29}$$

Upon substituting into Equation 28, we obtain

$$\begin{aligned} A_{\mathrm{PA}} &\approx \frac{1-2^{\frac{B_{\mathrm{CDI}}}{N_c(n_t-1)}}}{N_c} \\ &+ \frac{1-2^{\frac{B_{\mathrm{CDI}}}{N_c(n_t-1)}}}{N_c^2}\underbrace{\sum_{n=1}^{N_c}\sum_{k>n}^{N_c}\mathbb{E}[\cos(\Delta\xi_n-\Delta\xi_k)]}_{\eta}. \end{aligned} \tag{30}$$

In the following, we derive the closed-form expression of η. From Equation 25, we can see that if we normalize all the PAs with a certain PA, say first PA $e^{j\xi_1}$, the quantization accuracy of the global CDI will not change. This indicates that the first PA can be equivalently viewed as perfectly quantized, i.e., $\Delta\xi_1=0$. Hence, we have

$$\eta=\sum_{n=2}^{N_c}\sum_{k>n}^{N_c}\mathbb{E}[\cos(\Delta\xi_n-\Delta\xi_k)]+\sum_{n=2}^{N_c}\mathbb{E}[\cos\Delta\xi_n]. \tag{31}$$

For the considered worst case of $\alpha_1=\ldots=\alpha_{N_c}$, to quantize the N_c-1 PAs, the number of bit for quantizing each PA is

$$b_{\mathrm{PA}}=\frac{B_{\mathrm{PA}}}{N_c-1}. \tag{32}$$

Since the per-cell channels are isotropic, the PAs are uniformly distributed in $[0,2\pi]$ [15]. This indicates that it is optimal to quantize PA with a uniform scalar quantizer, and the quantization error of the nth PA is uniformly distributed within $[-\frac{\pi}{2^{b_{\mathrm{PA}}}},\frac{\pi}{2^{b_{\mathrm{PA}}}}]$. Then we have

$$\begin{aligned} \mathbb{E}[\cos(\Delta\xi_n)] &= \int_{-\pi/2^{b_{\mathrm{PA}}}}^{\pi/2^{b_{\mathrm{PA}}}}\frac{\cos x\times 2^{b_{\mathrm{PA}}}}{2\pi}\mathrm{d}x=\frac{2^{b_{\mathrm{PA}}}}{\pi}\sin(\frac{\pi}{2^{b_{\mathrm{PA}}}}), \\ \mathbb{E}[\sin(\Delta\xi_n)] &= \int_{-\pi/2^{b_{\mathrm{PA}}}}^{\pi/2^{b_{\mathrm{PA}}}}\frac{\sin x\times 2^{b_{\mathrm{PA}}}}{2\pi}\mathrm{d}x=0, n=2,\cdots,N_c, \end{aligned} \tag{33}$$

and

$$\begin{aligned} &\mathbb{E}[\cos(\Delta\xi_n-\Delta\xi_k)] \\ &=\mathbb{E}[\cos\Delta\xi_n]\,\mathbb{E}[\cos\Delta\xi_k]-\mathbb{E}[\sin\Delta\xi_n]\,\mathbb{E}[\sin\Delta\xi_k] \\ &=\frac{2^{2b_{\mathrm{PA}}}}{\pi^2}\sin^2(\frac{\pi}{2^{b_{\mathrm{PA}}}}), n\neq k\neq 1. \end{aligned} \tag{34}$$

Substituting Equation 34 into Equation 31, we obtain

$$\begin{aligned}\eta &= \sum_{n=2}^{N_c}\left(\frac{2^{b_{\mathrm{PA}}}}{\pi}\sin\left(\frac{\pi}{2^{b_{\mathrm{PA}}}}\right)+\sum_{k>n}^{N_c}\frac{2^{b_{\mathrm{PA}}}}{\pi^2}\sin^2\left(\frac{\pi}{2^{b_{\mathrm{PA}}}}\right)\right)\\ &= \frac{(N_c-1)2^{\frac{B_{\mathrm{PA}}}{N_c-1}}\sin\left(\frac{\pi}{2^{\frac{B_{\mathrm{PA}}}{N_c-1}}}\right)}{\pi}\\ &\quad\times\left(1+\frac{(N_c-2)2^{\frac{B_{\mathrm{PA}}}{N_c-1}}\sin\left(\frac{\pi}{2^{\frac{B_{\mathrm{PA}}}{N_c-1}}}\right)}{2\pi}\right).\end{aligned} \tag{35}$$

Substituted Equation 35 into Equation 30, the average global quantization accuracy can be approximated as

$$A_{\mathrm{PA}} \approx \left(1-2^{-\frac{B_{\mathrm{CDI}}}{N_c(n_t-1)}}\right)\times\frac{1}{N_c}\left(1+\frac{2\eta}{N_c}\right), \tag{36}$$

which is accurate when the following two conditions are met simultaneously: (1) $n_t \to \infty$, and (2) the per-cell codebook is well designed and $B_{\mathrm{CDI}} \to \infty$.

It is hard to compare the two strategies with and without the PA feedback directly from Equations 23 and 36 because the expression of η is complicated. To gain some insight, we consider that the number of bits for the PA is sufficiently large. In this case, we have $\lim_{B_{\mathrm{PA}}\to\infty}\eta = \frac{N_c(N_c-1)}{2}$. Upon substituting into Equation 36, we obtain

$$\lim_{B_{\mathrm{PA}}\to\infty} A_{\mathrm{PA}} = 1-2^{-\frac{B_{\mathrm{CDI}}}{N_c n_t - N_c}}. \tag{37}$$

Define the average quantization performance gain brought by the PA feedback as $G_{\mathrm{PA}} \triangleq A_{\mathrm{PA}} - A_{\mathrm{NPA}}$. We have

$$\lim_{B_{\mathrm{PA}}\to\infty} G_{\mathrm{PA}} = 2^{-\frac{B_{\mathrm{CDI}}}{N_c n_t - 1}} - 2^{-\frac{B_{\mathrm{CDI}}}{N_c n_t - N_c}} > 0. \tag{38}$$

The value of $\lim_{B_{\mathrm{PA}}\to\infty} G_{\mathrm{PA}}$ increases with N_c. However, if n_t is large, the impact of N_c will reduce. This means that the performance gain from the PA feedback is not significant for the systems with larger n_t and small N_c.

6 Simulation and numerical results

In this section, we validate previous analysis where several approximations were introduced and show the necessity for feeding back the per-cell channel norms and the PA by simulations in practical system settings. We consider a homogeneous cellular network and evaluate the performance of a reference cooperative cluster, which consists of N_c cells [17]. To reduce the complexity of simulation, instead of generating multiple interfering cells, we model the interference from the surrounding cells of the cluster as white noise, which is the worst-case interference and results in pessimistic performance [18]. To show the impact of CDI quantization, the cell-edge SNR is set as 10 dB, such that the system operating in multi-user interference limited the region unless otherwise specified. The users are distributed within a cell-edge region, satisfying $\alpha_{i_L}^2 / \max_{n\neq i_L}\alpha_n^2 < 6$ dB since cell-edge users prefer CoMP transmission, where α_{i_L} is the large-scale fading gain of a user with its master BS i_L and $\alpha_n, n \neq i_L$ are the gains with the coordinated BSs.

Since when orthogonal frequency division multiplexing (OFDM) systems are considered, each subcarrier is subject to flat fading, we consider a frequency-flat fading channel. All our analysis and results can then be extended to OFDM systems. The small-scale fading channels between the user and each coordinated BS are i.i.d. Rayleigh channels. All of the results are obtained from 1,000 trails of Monte Carlo simulations, where both user locations and small-scale fading channels are randomly generated.

The layout of the reference cooperative cluster is set according to [17], including the cell radius, the number and distribution of candidate users, and the path loss model, which are listed with other simulation parameters in Table 1. In practice, the quantization of global CDI and global channel norm at the user will be based on channel estimation, which is never perfect. Nonetheless, the simulation results with channel estimation errors are similar as those without errors, which are not shown for conciseness. The SUS is performed at the CU with the quantized global norm and global CDI, and the zero-forcing beamforming is computed with the quantized CDI, i.e., the reconstructed global CDI with Equation 5. To evaluate the impact of PBPC on the performance, we consider a simple power allocation satisfying PBPC [1]. Specifically, the overall transmit power of the coordinated BS is first equally allocated to the selected users. Then, if the transmit power of a BS exceeds the maximal power,

Table 1 The simulation parameters

Parameter	Value/description
Number of antennas per user	1
Cell radius	250 m
Path loss model (dB)	$36.3 + 37.6\log(D)$, where D is the distance from a user to a BS
Number of users in each cell	10
Distribution of the users	Randomly distributed within cell-edge region
Per-cell codebook	4-bit [17] RVQ codebook [19]
Feedback error and delay	None
Beamformer	Zero-forcing beamforming
Scheduling method	SUS with the orthogonality threshold as 0.3

the power allocated to multiple users will decrease at the same time to reduce the transmit power of the BS to the maximal power. The per-user data rate is calculated with the SINR estimate shown in Equation 15. When the estimated SINR exceeds the actual SINR, an outage happens, then the data rate is set to 0 bps/Hz in our simulations.

6.1 Feedback of global quantization accuracy

As analyzed in Section 3, the global quantization accuracy $\cos\theta_m$ should be fed back for the CU to estimate the CQI. We first show how many bits are required to quantize $\cos\theta_m$.

The codebook for quantizing $\cos\theta_m$ is generated by Lloyd's algorithm [12]. Denote its quantized version as $\hat{\cos}\,\theta_m$, which is defined as the lower end of the quantization interval that includes $\cos\theta_m$, similar to Equation 16. This ensures that $\hat{\cos}\,\theta_m \leq \cos\theta_m$, which avoids the outage led by the inaccuracy of the quantization of $\cos\theta_m$.

We consider $N_c = 3$ and $n_t = 4$. To emphasize the impact of $\cos\theta_m$ quantization here, the global channel norm $||\mathbf{g}_m||$ and the noise and inter-cluster interference variance σ_m^2 are assumed to be perfectly known at the CU when estimating the CQI with Equation 15. The codewords for quantizing the per-cell CDIs are selected jointly with Equation 9, and the feedback of PA is not considered.

The legends '1-bit Quan.', '2-bit Quan.', '3-bit Quan.', and '4-bit Quan.' represent the results when $\cos\theta_m$ is quantized with 1, 2, 3, and 4 bits, respectively. The legend 'Quan.' is for the results of quantized $\cos\theta_m$ with different numbers of bits, and 'Perfect Quan.' is for the result when $\cos\theta_m$ is not the quantization error.

As shown in Figure 1a, the outage probability is 0 when using the CQI estimated with Equation 15, which however leads to a rate loss from that with perfectly quantized $\cos\theta_m$. As shown in Figure 1b, with a 4-bit quantization, the rate loss is less than 6%. In the rest of the simulations, we use 4 bits for quantizing $\cos\theta_m$.

6.2 Necessity of per-cell norm feedback

6.2.1 Impact on CQI estimation

To show the impact of the channel norm feedback mechanisms on the CQI estimation, in Figure 2a, we simulate the CDFs of the estimated SINR and quantized global channel norm with two feedback mechanisms: feeding back per-cell channel norms or global channel norm. The total number of bits is set as 6 or 18, then the number of bits for

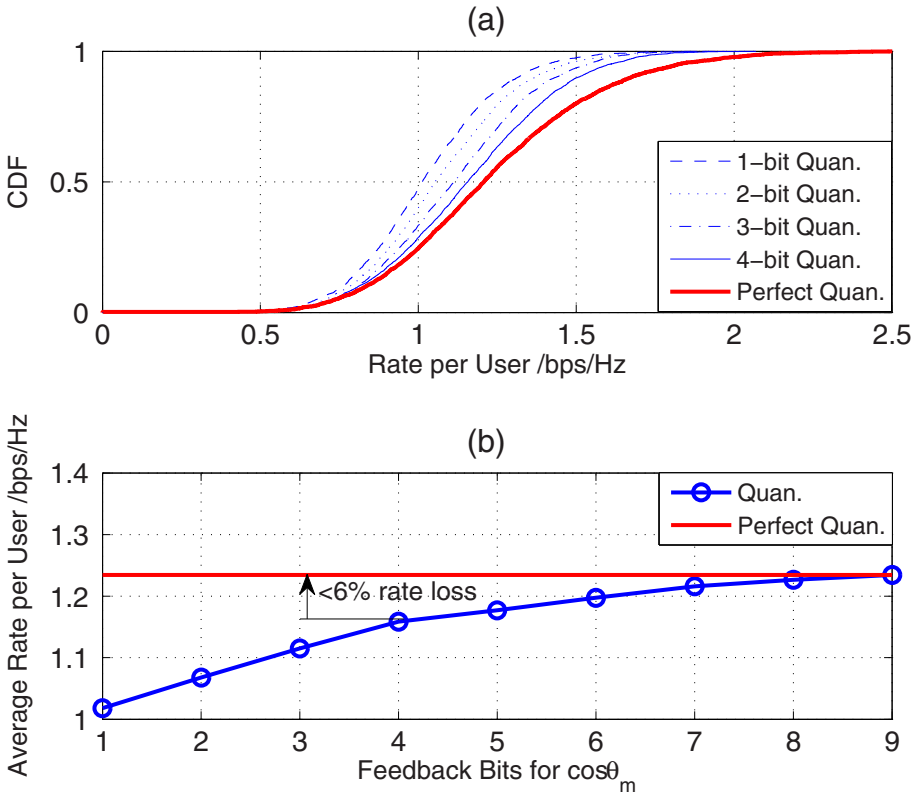

Figure 1 Per-user data rate with different quantization bits for $\cos\theta_m$. (a) CDF of per-user data rate when $\cos\theta_m$ is quantized with different numbers of bits. **(b)** The average per-user data rate when $\cos\theta_m$ is quantized with different numbers of bits.

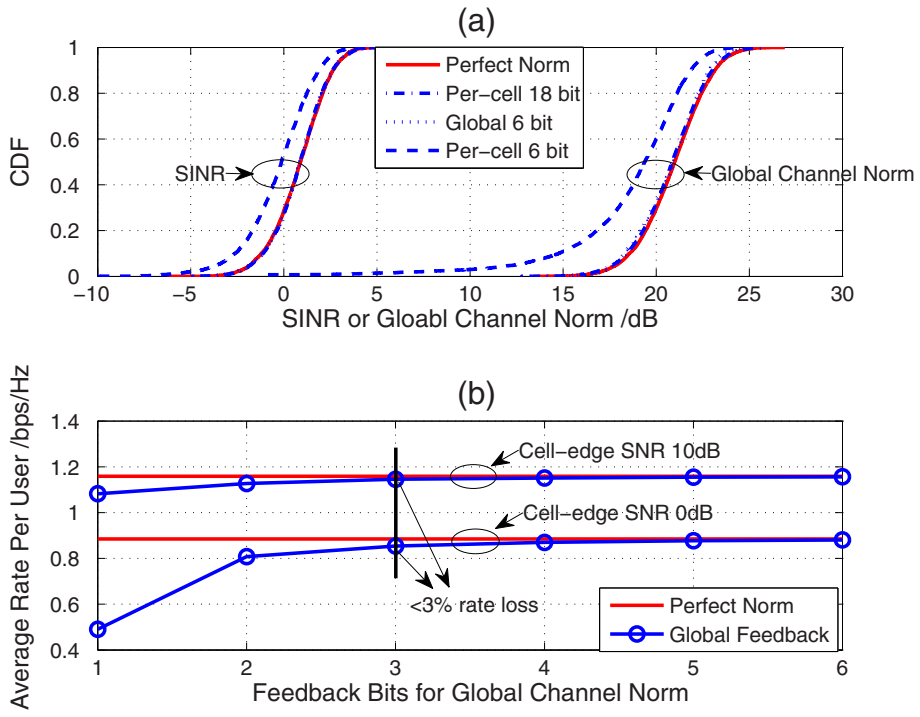

Figure 2 SINR and average per-user data rate with different quantization mechanisms for channel norm. (a) The CDF of global channel norm and SINR for two feedback mechanisms under 10-dB cell-edge SNR, where the result of 'Perfect Norm', 'Global 6 bit', and 'Per-cell 18 bit' overlap with each other. **(b)** The average data rates achieved using the perfect and quantized global channel norms, under both 0- and 10-dB cell-edge SNR.

each per-cell channel norm $\frac{6}{N_c} = 2$ or 6. The codebooks for quantizing both the per-cell and global channel norm are generated by Lloyd's algorithm [12]. The legend 'Global 6 bit' is for the case using global channel norm with 6-bit quantization and 'Per-cell 6 bit' and 'Per-cell 18 bit' are for the cases using the 2-bit and 6-bit per-cell channel norm quantization, respectively. The codewords for per-cell CDIs are selected jointly with Equation 9, and the PA is not fed back. Again, we consider $N_c = 3$ and $n_t = 4$.

The comparisons between the two feedback mechanisms for the global channel norm quantization are consistent with the previous analysis. The results validate that the global channel norm-based feedback strategy achieves the same performance as the per-cell channel norm-based strategy with $\frac{1}{N_c}$ times of feedback overhead. The performance gap of the SINRs estimated with the per-cell channel norm and the global channel norm is less than the gap of the quantized global channel norm. This is because the multi-user interference dominates in the SINR estimate under the 10-dB cell-edge SNR.

To show how many bits are needed for quantizing the global channel norm, in Figure 2b, we simulate the average per-user rate achieved using the perfect global channel norm (with legend 'Perfect Norm') and the global channel norm quantized with different bits (with legend 'Global Feedback'). Except for the 10-dB cell-edge SNR, we also consider 0-dB cell-edge SNR, which represents the noise limited case. It shows that in both scenarios, 3 bits is enough for quantizing the global channel norm to ensure the average rate loss less than 3% of that with perfect global channel norm.

6.2.2 *Impact on global CDI reconstruction*

To show the impact of the per-cell channel norm feedback on the global CDI reconstruction, we compare the performance of the reconstruction methods only with the large-scale fading gains in Equation 5 (with legend 'Recons. w large scale') and with the composite per-cell channel norm $\alpha_{m,n}||\hat{\mathbf{h}}_{m,n}||$, where the per-cell channel norms are quantized individually at each user. The legends 'Recons. w perfect norm' and 'Recons. w 3-bit per norm' respectively represent the reconstruction methods with perfect composite per-cell channel norms and the per-cell channel norms each quantized with 3 bits. Considering that the simulation is very slow with large values of N_c and n_t, we use the statistics of RVQ [19] to reflect the quantization performance of the scheme with independent codeword selection, where the PA is either unknown or perfectly known to the CU in the reconstruction.

As shown in Figure 3, the average rate loss due to the reconstruction without using the per-cell channel

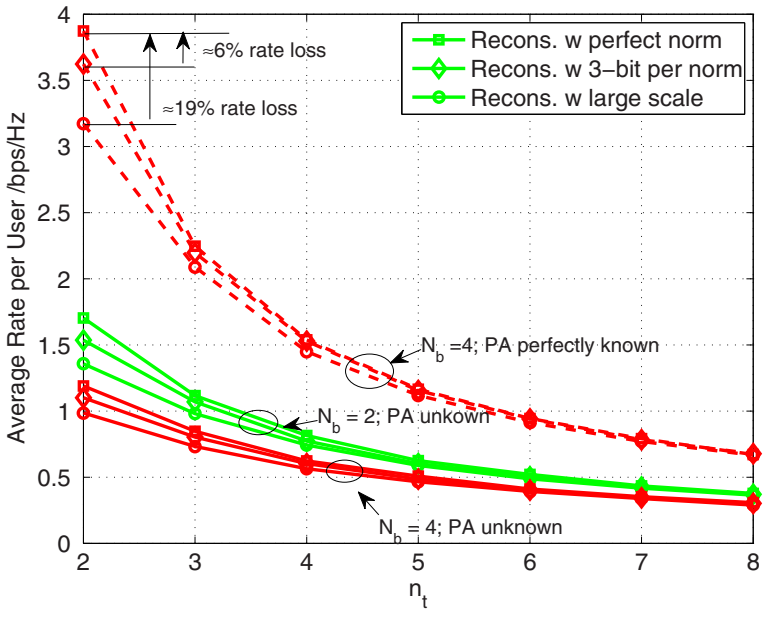

Figure 3 Average per-user data rate with different global CDI reconstruction methods.

norms reduces with the increase of n_t, and $n_t \geq 4$ is enough to ensure that the reconstruction method with Equation 5 achieves the same performance with perfect per-cell channel norms. This validates our previous analysis. However, the rate loss becomes evident with small n_t, e.g., $n_t = 2$, especially when the PAs are perfectly fed back. It is because, in this case, the reconstruction without the per-cell channel norms becomes the bottleneck in improving the quantization performance of the global CDI, and at least 3 bits is necessary for each per-cell channel norm to compensate the rate loss. This suggests that the per-cell channel norms are not necessary to be fed back for reconstructing the global CDI when $n_t \geq 4$ or N_c is small, which is typical for practical CoMP systems.

6.3 Necessity of PA feedback

6.3.1 Accuracy of the approximations

Before showing the necessity of PA feedback, we first evaluate the accuracy of the approximations introduced in deriving the average quantization accuracy with and without PA quantization by simulations.

Consider the worst case $\alpha_1 = \ldots = \alpha_{N_c}$ in the simulations as in the analysis. To ensure an accurate approximation of A_{PA}, a large value of n_t is required. We set $n_t = 2, 4$, which are typical configurations of the LTE standard [17]. As for the approximation of A_{NPA}, $N_c \times n_t$ needs to be large enough. We consider a CoMP system with three coordinated BSs where $N_c \times n_t = 6, 12$ to evaluate the accuracy of the approximations.

The simulation results for the average global quantization accuracy with and without the PA feedback are respectively with legends A_{PA} and A_{NPA}. The approximated average quantization accuracy with and without PA feedback are numerically computed with Equations 36 and (23), respectively, with legends 'Appro. of A_{PA}' and 'Appro. of A_{NPA}'.

As shown in Figure 4, the approximations are accurate for the considered cases. The larger values of $N_c \times n_t$ and n_t provide more accurate approximations.

6.3.2 Necessity of the PA feedback

We evaluate the necessity of PA feedback by comparing the numerical results of the average global quantization accuracy with and without the PA feedback and the simulation results of the average per-user rate with and without the PA feedback. The total number of bits for the per-cell CDI feedback is $4 \times N_c$ bits, and the PA feedback needs extra B_{PA} bits. Considering the prohibited complexity of joint codeword selection, we use serial codeword selection [6] in the simulation, which performs close to the joint codeword selection but with much lower complexity. Since the feedback of PA only decides the global CDI quantization, we use the perfect global channel norm of each user to compute the CQI in the following simulation. The reconstruction method shown in Equation 5 is considered.

The numerical results of the average global quantization accuracy of the strategies with and without the PA feedback are shown in Figure 5a, where Appro. of A_{NPA}

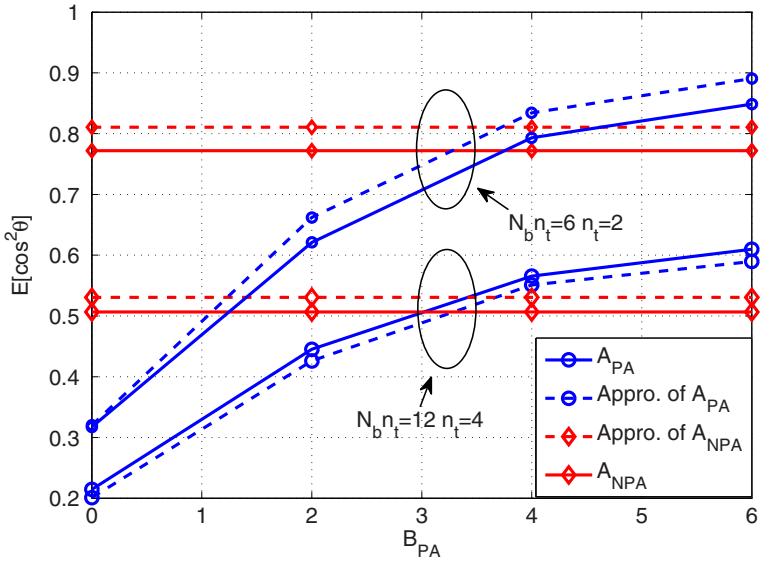

Figure 4 The accuracy of the approximated A_{NPA} and A_{PA} with $N_c = 3$ and $n_t = 2, 4$.

and Appro. of A_{PA} are obtained with Equations 23 and 36. To show how the gain in average global quantization accuracy affects the performance of the system, the simulation results of the average per-user data rate with and without the PA feedback are shown in Figure 5b, where 'R_{NPA}' and 'R_{PA}' are the average data rate per user with and without PA feedback, respectively. As a performance baseline, we also show the performance of non-CoMP systems with legend '$R_{\mathrm{non-CoMP}}$' in the case of $N_c = 3$ and $n_t = 2$, where, in other scenarios, the comparison results are similar. For a fair comparison, the users are located within 6-dB cell-edge region in non-CoMP systems. It shows that B_{PA} should be large enough to provide an evident performance gain from the PA feedback, in terms of both the average global quantization accuracy and the average per-user data rate. Moreover,

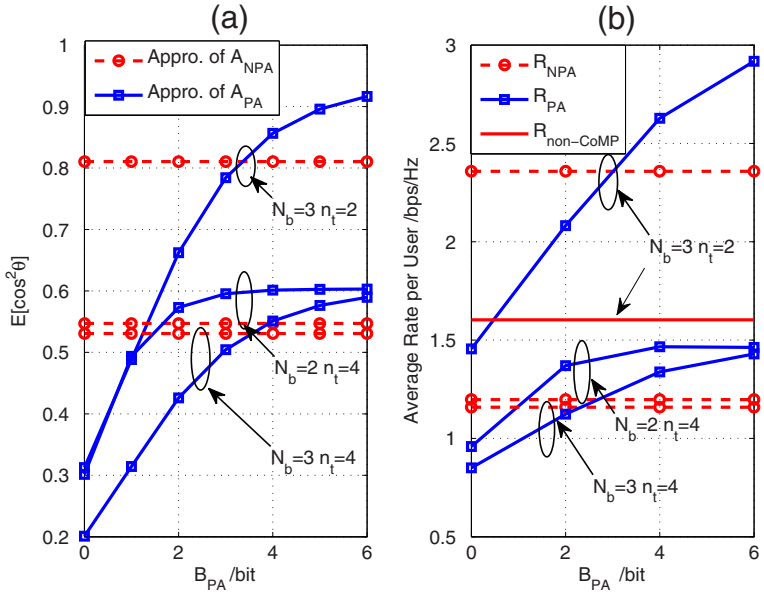

Figure 5 Global quantization accuracy and per-user data rate for the methods with and without PA feedback. (a) The numerical results of the average global quantization accuracy with and without the PA feedback. **(b)** The simulation results of the average per-user rate with and without the PA feedback.

the gain becomes smaller with less coordinated BSs and more antennas at each BS, which validates the previous analysis.

In Figure 6, we show the simulation results of the average per-user rate gain provided by the PA feedback, which is defined as $\frac{R_{\mathrm{PA}}-R_{\mathrm{NPA}}}{R_{\mathrm{NPA}}}$, with $1 \sim 3$ bits for each PA. It shows that at least 2 bits is required for feeding back each PA to bring a per-user rate gain. The maximal per-user rate gains are $21\% \sim 26\%$ in the cases of $n_t = 2$ and $N_c = 2 \sim 5$ with 3 bits for quantizing each PA, but the feedback overhead needs to increase $37.5\% \sim 60\%$ of that without the PA feedback.

7 Conclusions

In this paper, we investigated what should be fed back in per-cell codebook-based limited feedback CoMP systems to facilitate the coherent downlink cooperative transmission. We first presented a conservative CQI estimation method aiming at reducing the outage probability. To estimate the CQI at the CU, the global CDI and the corresponding quantization accuracy, the global channel norm, and the noise and inter-cluster interference variance need to be fed back. Considering that both the global channel norm and the global CDI reconstruction depend on the per-cell channel norms, we analyzed if these norms need to be fed back by deriving the average quantization performance of the global channel norm and the asymptotic weighting factors in the global CDI with and without the per-cell channel norms. To show if the PA feedback is necessary, we derived the approximated average quantization accuracy of the reconstructed global CDI using the joint codeword selection without PA feedback and the independent codeword selection with PA feedback. We used simulation and numerical results to evaluate the accuracy of the approximations and show that the conclusions drawn from the average quantization accuracy are also true for the average per-user data rate. The following observations were obtained from the analytical and simulation results: (1) the per-cell instantaneous channel norms are unnecessary to be fed back; (2) the global quantization accuracy and the global channel norm need to be fed back, which respectively require 4 and 3 bits for the typical setting of $N_c = 3$ and $n_t = 4$; and (3) the performance gain provided by the PA feedback is not significant when N_c is small and n_t is large. Considering that the extra overhead exceeds the per-user rate gain from feeding back the PA, using the joint codeword selection without PA feedback may be more desirable than using the independent selection with PA feedback.

Appendix 1

Proof of Proposition 1. We consider high-resolution quantization, which implies that (1) the number of quantization bits, B_h, is infinite and (2) the quantization interval is small compared to the quantization range of Y_n, $[\delta_1, \delta_2]$

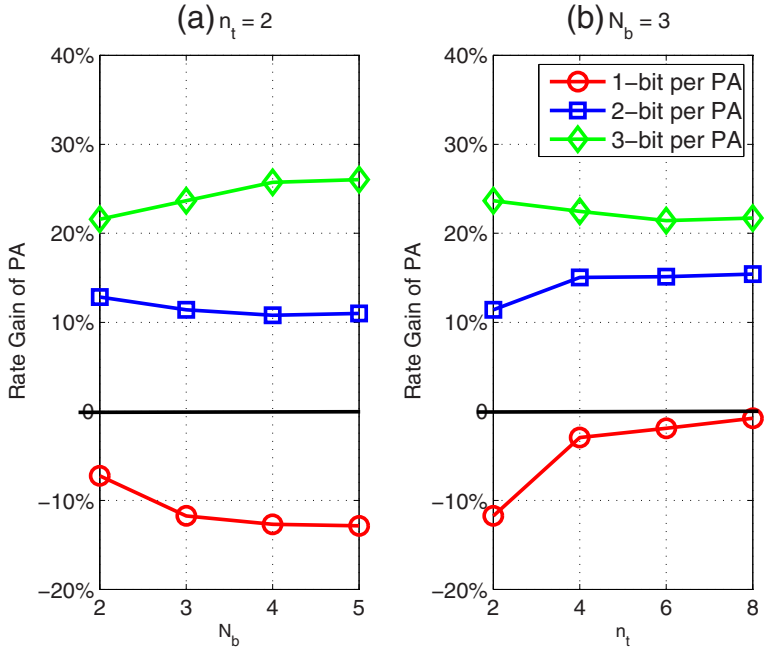

Figure 6 The performance gain in average per-user rate provided by the PA feedback. (a) The average per-user rate gain with $n_t = 2$. **(b)** The average per-user rate gain with $N_b = 3$.

[12]. According to the second assumption, i.e., the quantization interval is small, we can derive

$$\begin{aligned}\mathbb{E}[Y_n^2]-\mathbb{E}[\hat{Y}_n^2] &\approx \sum_{j=1}^{2^{B_\mathrm{h}}}\left[(y^{(j+1)})^2-(y^{(j)})^2\right]\int_{y^{(j)}}^{y^{(j+1)}} f(y)\mathrm{d}y \\ &= \sum_{j=1}^{2^{B_\mathrm{h}}}(y^{(j+1)}-y^{(j)})(y^{(j+1)}+y^{(j)})P_j,\end{aligned} \tag{39}$$

where $P_j \triangleq \int_{y^{(j)}}^{y^{(j+1)}} f(y)\mathrm{d}y$.

According to [12], under the assumption of high-resolution quantization, the performance of any quantization method can be approximated by the uniform quantization with the same bits; hence, the quantization interval is $y^{(j+1)}-y^{(j)} \approx \frac{2(\delta_2-\delta_1)}{2^{B_\mathrm{h}}-1}$. Then we have

$$\begin{aligned}\mathbb{E}[Y_n^2]-\mathbb{E}[\hat{Y}_n^2] &\approx \sum_{j=1}^{2^{B_\mathrm{h}}}\frac{\delta_2-\delta_1}{2^{B_\mathrm{h}}-1}(2y^{(j)}+\frac{\delta_2-\delta_1}{2^{B_\mathrm{h}}-1})P_j \\ &= \frac{2(\delta_2-\delta_1)}{2^{B_\mathrm{h}}-1}\sum_{j=1}^{2^{B_\mathrm{h}}}y^{(j)}P_j+\frac{(\delta_2-\delta_1)^2}{(2^{B_\mathrm{h}}-1)^2}\sum_{j=1}^{2^{B_\mathrm{h}}}P_j.\end{aligned} \tag{40}$$

Based on the property of the integral, we have

$$\begin{aligned}\sum_{j=1}^{2^{B_\mathrm{h}}}y^{(j)}P_j &= \sum_{j=1}^{2^{B_\mathrm{h}}}\int_{y^{(j)}}^{y^{(j+1)}}y^{(j)}f(y)\mathrm{d}y = \int_{y^{(1)}}^{y^{(2^{B_\mathrm{h}}+1)}}y^{(j)}f(y)\mathrm{d}y \\ &= \int_{\delta_1}^{\infty}y^{(j)}f(y)\mathrm{d}y, \\ \sum_{j=1}^{2^{B_\mathrm{h}}}P_j &= \sum_{j=1}^{2^{B_\mathrm{h}}}\int_{y^{(j)}}^{y^{(j+1)}}f(y)\mathrm{d}y = \int_{y^{(1)}}^{y^{(2^{B_\mathrm{h}}+1)}}f(y)\mathrm{d}y \\ &= \int_{\delta_1}^{\infty}f(y)\mathrm{d}y.\end{aligned} \tag{41}$$

We assume $\mathrm{P}[\delta_1 \le Y_n \le \delta_2] \approx 1$, which implies $\mathrm{P}[Y_n \le \delta_1] \approx 0$. Therefore, we have

$$\begin{aligned}\sum_{j=1}^{2^{B_\mathrm{h}}}y^{(j)}P_j &\approx \int_0^{\infty}y^{(j)}f(y)\mathrm{d}y = \mathbb{E}[Y_n], \\ \sum_{j=1}^{2^{B_\mathrm{h}}}P_j &\approx \int_0^{\infty}f(y)\mathrm{d}y = 1.\end{aligned} \tag{42}$$

Upon substituting into Equation 40, we obtain

$$\mathbb{E}[Y_n^2]-\mathbb{E}[\hat{Y}_n^2] \approx \frac{2(\delta_2-\delta_1)}{2^{B_\mathrm{h}}-1}\mathbb{E}[Y_n]+\frac{(\delta_2-\delta_1)^2}{(2^{B_\mathrm{h}}-1)^2}. \tag{43}$$

The approximation is accurate when the value of B_h is large.

Appendix 2

Proof of Proposition 2. Based on the property of variance, we can derive

$$\begin{aligned}\mathrm{Var}(\frac{||\mathbf{h}_n||^2}{n_t}) &= \frac{1}{n_t^2}\sum_{j=1}^{n_t}\mathrm{Var}(|h_{n,j}|^2) \\ &= \frac{1}{n_t^2}\times n_t = \frac{1}{n_t}, n=1,\cdots,N_c,\end{aligned} \tag{44}$$

which indicates that the variance of normalized per-cell channel energy $\frac{||\mathbf{h}_n||^2}{n_t}$ approaches zero with large n_t, and $\frac{||\mathbf{h}_n||^2}{n_t}$ approaches a constant, whose value is the same as $\mathbb{E}[|h_{n,j}|^2]$ since the per-cell channels are assumed as i.i.d..

For the per-cell channels with arbitrary distribution, when n_t is sufficiently large, we obtain

$$\begin{aligned}\mathbb{E}[||\mathbf{g}||] &= \mathbb{E}\left[\sqrt{\sum_{n=1}^{N_c}n_t\alpha_n^2\frac{||\mathbf{h}_n||^2}{n_t}}\right] \\ &\approx \mathbb{E}\left[\sqrt{\sum_{n=1}^{N_c}n_t\alpha_n^2}\times\sqrt{\frac{||\mathbf{h}_n||^2}{n_t}}\right] \\ &= \sqrt{\sum_{n=1}^{N_c}n_t\alpha_n^2}\times\frac{\mathbb{E}[||\mathbf{h}_n||]}{\sqrt{n_t}} = \sqrt{\sum_{n=1}^{N_c}\alpha_n^2}\times\mathbb{E}[||\mathbf{h}_n||].\end{aligned} \tag{45}$$

Appendix 3

Proof of Proposition 3. To prove this proposition, in the following, we will prove that $\lim_{n_t\to\infty}g_n \to \hat{g}_n$ with probability 1, i.e., $P[\lim_{n_t\to\infty}g_n=\hat{g}_n]=1$.

We start by proving a lemma.

Lemma 1. *Given two constants $\bar{a},\bar{b}>0$, and two non-negative random series $\{a_n\}$ and $\{b_n\}$ where $\{b_n\}$ is lower bounded by $B>0$, i.e., $b_n \ge B, \forall n$. If $\{a_n\}$ approaches $\bar{a}$ with probability 1 and $\{b_n\}$ approaches $\bar{b}$ with probability 1, i.e., $P[\lim_{n\to\infty}a_n=\bar{a}]=1$ and $P[\lim_{n\to\infty}b_n=\bar{b}]=1$, then $\{\frac{a_n}{b_n}\}$ approaches $\frac{\bar{a}}{\bar{b}}$ with probability 1, i.e.,*

$$P\left[\lim_{n\to\infty}\frac{a_n}{b_n}=\frac{\bar{a}}{\bar{b}}\right]=1.$$

Proof. To prove $P[\lim_{n\to\infty}\frac{a_n}{b_n}=\frac{\bar{a}}{\bar{b}}]=1$, we need to prove $\forall\varepsilon>0$, $\exists N$, which makes $P[|\frac{a_n}{b_n}-\frac{\bar{a}}{\bar{b}}|\le\varepsilon]>1-\varepsilon$ with $n>N$.

First, we have

$$\begin{aligned}&\left|\frac{a_n}{b_n}-\frac{\bar{a}}{\bar{b}}\right| \\ &=\frac{|\bar{b}a_n-\bar{a}\bar{b}-(\bar{a}b_n-\bar{a}\bar{b})|}{\bar{b}b_n}\overset{(1)}{\leq}\frac{\bar{b}|a_n-\bar{a}|+\bar{a}|b_n-\bar{b}|}{\bar{b}b_n} \\ &\overset{(2)}{\leq}\frac{\bar{b}|a_n-\bar{a}|+\bar{a}|b_n-\bar{b}|}{\bar{b}B},\end{aligned} \tag{46}$$

where (1) comes from the triangle inequality, and (2) comes from the condition of $b_n \geq B$.

Then, for any $\varepsilon > 0$ we have

$$\begin{aligned}P\left[|\frac{a_n}{b_n}-\frac{\bar{a}}{\bar{b}}|\leq\varepsilon\right] &\geq P\left[\frac{\bar{b}|a_n-\bar{a}|+\bar{a}|b_n-\bar{b}|}{\bar{b}B}\leq\varepsilon\right] \\ &> P\left[\frac{|a_n-\bar{a}|}{B}<\varepsilon_1\right]\times P\left[\frac{\bar{a}|b_n-\bar{b}|}{\bar{b}B}<\varepsilon_2\right]\triangleq P_\varepsilon,\end{aligned} \tag{47}$$

where $\varepsilon_1, \varepsilon_2$ are non-negative numbers with $\varepsilon_1+\varepsilon_2=\varepsilon$.

Since $P[\lim_{n\to\infty} a_n = \bar{a}] = 1$, we can find N_1 which ensures

$$P[|a_n-\bar{a}|<B\varepsilon_1]>1-B\varepsilon_1, \tag{48}$$

when $n > N_1$ In the same manner, we can find N_2 which ensures

$$P\left[\frac{\bar{a}|b_n-\bar{b}|}{\bar{b}B}<\varepsilon_2\right]>1-\frac{B\bar{b}}{\bar{a}}\varepsilon_2, \tag{49}$$

when $n > N_2$.

Therefore, when $n > \max(N_1, N_2)$, by substituting Equations 48 and 49 into Equation 47, we obtain

$$P_\varepsilon>(1-B\varepsilon_1)(1-\frac{B\bar{b}}{\bar{a}}\varepsilon_2)=1-(B\varepsilon_1+\frac{B\bar{b}}{\bar{a}}\varepsilon_2-\frac{B^2\bar{b}}{\bar{a}}\varepsilon_1\varepsilon_2). \tag{50}$$

Define $\hat{\varepsilon} \triangleq \max(\varepsilon, B\varepsilon_1+\frac{B\bar{b}}{\bar{a}}\varepsilon_2-\frac{B^2\bar{b}}{\bar{a}}\varepsilon_1\varepsilon_2)$. Then, we obtain that $\forall\hat{\varepsilon}, \exists N=\max(N_1,N_2)$, which ensures

$$P\left[|\frac{a_n}{b_n}-\frac{\bar{a}}{\bar{b}}|\leq\hat{\varepsilon}\right]>1-\hat{\varepsilon},$$

when $n > N$. □

Now we prove the proposition. Actually, we only need to prove that the proposition satisfies all the conditions in Lemma 1, then the proposition is established based on the lemma.

Rewrite Equation 4 as follows:

$$g_n=\frac{\alpha_n\sqrt{\frac{\sum_{j=1}^{n_t}|h_{n,j}|^2}{n_t}}}{\sqrt{\sum_{n=1}^{N_c}\alpha_n^2\frac{\sum_{j=1}^{n_t}|h_{n,j}|^2}{n_t}}}. \tag{51}$$

Define a random variable $X_n \triangleq \frac{\sum_{j=1}^{n_t}|h_{n,j}|^2}{n_t}$. Since per-cell channels are assumed as i.i.d. and subject to $\mathcal{CN}(0,1)$, $|h_{n,j}|$ is subject to Rayleigh distribution with $\mathbb{E}[|h_{n,j}|^2]=1$ and is independent with each other. Based on the law of large numbers, we have $P\left[\lim_{n_t\to\infty} X_n = \mathbb{E}[|h_{n,j}|^2]\right]=1$. Since $\mathbb{E}[|h_{n,j}|^2]=1$, we have $P\left[\lim_{n_t\to\infty} X_n=1\right]=1$, i.e., X_n approaches 1 with probability 1 when n_t goes to infinity. Based on the property of limitation, it is easy to prove that $P\left[\lim_{n_t\to\infty}\sqrt{X_n}=1\right]=1$. Then we have

$$P[\lim_{n_t\to\infty}\alpha_n\sqrt{X_n}=\alpha_n]=1. \tag{52}$$

Again, based on the property of limitation, we have $\lim_{n_t\to\infty}\sqrt{\sum_{n=1}^{N_c}\alpha_n^2X_n}=\sqrt{\sum_{n=1}^{N_c}\alpha_n^2\lim_{n_t\to\infty}X_n}$. Since $P\left[\lim_{n_t\to\infty}X_n=1\right]=1$ and all the X_n are independent, we can derive

$$P\left[\lim_{n_t\to\infty}\sqrt{\sum_{n=1}^{N_c}\alpha_n^2X_n}=\sqrt{\sum_{n=1}^{N_c}\alpha_n^2}\right]=1. \tag{53}$$

It means that the numerator and denominator respectively approach a constant with probability 1.

It is reasonable to assume that $X_n, n=1,\ldots,N_c$ are lower bounded by $\underline{X}>0$. Substituting into the denominator of g_n, it is easy to derive that the denominator also has a lower bound, which is $\sqrt{\sum_{n=1}^{N_c}\alpha_n^2X_n}\geq\sqrt{\sum_{n=1}^{N_c}\alpha_n^2\underline{X}}$.

Then based on Lemma 1, we obtain that $P[\lim_{n_t\to\infty}g_n=\frac{\alpha_n}{\sqrt{\sum_{n=1}^{N_c}\alpha_n^2}}]=1$, i.e.,

$$P[\lim_{n_t\to\infty}g_n=\hat{g}_n]=1. \tag{54}$$

It indicates that $g_n\approx\hat{g}_n$ when $n_t\to\infty$.

Competing interests
The authors declare that they have no competing interests.

Received: 4 January 2013 Accepted: 28 August 2013
Published: 18 September 2013

References

1. MK Karakayali, GJ Foschini, RA Valenzuela, Network coordination for spectrally efficient communications in cellular systems. IEEE Wireless Commun. Mag. **13**(4), 56–61 (2006)

2. D Gesbert, S Hanly, H Huang, S Shamai, O Simeone, W Yu, Multi-cell MIMO cooperative networks: a new look at interference. IEEE J. Sel. Areas Commun. **28**(9), 1380–1408 (2010)
3. DJ Love, RW Heath, VKN Lau, D Gesbert, BD Rao, M Andrews, An overview of limited feedback in wireless communication systems. IEEE J. Sel. Areas Commun. **26**(8), 1341–1365 (2008)
4. T Yoo, N Jindal, A Goldsmith, Multi-antenna downlink channels with limited feedback and user selection. IEEE J. Sel. Areas Commun. **25**, 1478–1491 (2007)
5. Y Cheng, VKN Lau, Y Long, A scalable limited feedback design for network MIMO using per-cell product codebook. IEEE Trans. Wireless Commun. **9**(10), 3093–3099 (2010)
6. X Hou, C Yang, *Codebook design and selection for multi-cell cooperative transmission limited feedback systems. IEEE VTC, Budapest, 15–18 May 2011* (IEEE, Piscataway, 2011), pp. 1–5
7. D Su, X Hou, C Yang, *Quantization based on per-cell codebook in cooperative multi-cell systems. IEEE WCNC, Cancun, 28–31 March 2011* (IEEE, Piscataway, 2011), pp. 1753–1758
8. F Yuan, C Yang, Bit allocation between per-cell codebook and phase ambiguity quantization for limited feedback coordinated multi-point transmission systems. IEEE Trans. Commun. **60**(9), 2546–2559 (2012)
9. K Huang, JG Andrews, RW Heath, Performance of orthogonal beamforming for SDMA with limited feedback. IEEE Trans. Veh. Tech. **58**, 152–164 (2009)
10. RA Horn, CR Johnson, *Matrix Analysis* (Cambridge University Press, Cambridge, 1990)
11. B Khoshnevis, W Yu, Bit allocation law for multiantenna channel feedback quantization: single-user case. IEEE Trans. Signal Process. **59**(5), 2270–2283 (2011)
12. A Gersho, RM Gray, *Vector Quantization and Signal Compression* (Kluwer, Boston, 1992)
13. D Su, C Yang, *Necessity of phase ambiguity quantization for limited feedback coordinated multi-point transmission. IEEE VTC, San Francisco, 5–8 Sept 2011* (IEEE, Piscataway, 2011), pp. 1–5
14. S Zhou, Z Wang, GB Giannakis, Quantifying the power loss when transmit beamforming relies on finite-rate feedback. IEEE Trans. Wireless Commun. **4**(4), 1948–1957 (2005)
15. BM Hochwald, TL Marzetta, Unitary space-time modulation for multiple-antenna communications in rayleigh flat fading. IEEE Trans. Inf. Theory. **46**(2), 543–564 (2000)
16. DJ Love, RW Heath, T Strohmer, Grassmannian beamforming for multiple-input multiple-output wireless systems. IEEE Trans. Inf. Theory. **49**(10), 2735–2747 (2003)
17. 3GPP, 3rd Generation partnership project; technical specification group radio access network; coordinated multi-point operation for LTE physical layer aspects (Release 11). TS 36.819 v11.1.0 (2011). http://www.3gpp.org Accessed 12 Sep. 2012
18. H Huang, M Trivellato, A Hottinen, M Shafi, P Smith, RA Valenzuela, Increasing downlink cellular throughput with limited network MIMO coordination. IEEE Trans. Wireless Commun. **8**(6), 2983–2989 (2009)
19. N Jindal, MIMO broadcast channels with finite-rate feedback. IEEE Trans. Inf. Theory. **52**(11), 5045–5060 (2006)

doi:10.1186/1687-1499-2013-232
Cite this article as: Su and Yang: **What should be fed back for per-cell codebook-based limited feedback coordinated multi-point systems?** *EURASIP Journal on Wireless Communications and Networking* 2013 **2013**:232.

Submit your manuscript to a SpringerOpen journal and benefit from:

► Convenient online submission
► Rigorous peer review
► Immediate publication on acceptance
► Open access: articles freely available online
► High visibility within the field
► Retaining the copyright to your article

Submit your next manuscript at ► springeropen.com